Vietnam Journal of Science and Technology ***59*** *(6A) (2021) 79-91*

doi:10.15625/2525-2518/59/6A/16383

NUMERICAL SIMULATION OF THE STRESS-STRAIN DURING CONSTRAINED GROOVE PRESSING PROCESS

Pham Quang[1, *], Pham Thi Thuy[2], Dang Thi Hong Hue[1], Hoang Thi Ngoc Quyen[1], Tran Thi Thu Hien[1], Dao Minh Ngung[1]

[1]*School of Material Science and Engineering, Hanoi University of Science and Technology, No.1 Dai Co Viet, Ha Noi, Viet Nam*

[2]*Falcuty of Electro - Mechanics, Hanoi University of Mining and Geology, 18 Pho Vien, Bac Tu Liem, Ha Noi, Viet Nam*

[*]Email: *quang.pham@hust.edu.vn*

Received: 15 August 2021; Accepted for publication: 14 January 2022

Abstract. In the case of plane deformation, the stress-strain of the workpiece can be calculated analytically with some simplifications without losing the generality of the problem. Numerical simulation by DEFORM software can be used to analyze most thermo-mechanical forming processes, and many heat treatment processes. The sequentially simulate each process that is to be applied to the workpiece of Constrained Grooved Pressing (CGP) plastic deformation process by finite element method allows to determine technological parameters such as pressure force, stress field, strain field and risk of failure or destruction. The stress-strain has been analyzed at the characteristic points of the plastic deformation region including on the surface, at the center of the workpiece and at the transition regions, the results are consistent with the theoretical study. The unique feature of CGP technology compared to other types of severe plastic deformation (SPD) is that the plastic deformation zone is not in a direct contact with the mold surface, but subjected to indirect forces, and has a small hydrostatic stress. The hydrostatic force and stress parameters only come into play at the end of the back elastic compression stroke. Through numerical simulation, it is possible to visually determine the state of stress and strain on the entire workpiece at all times of the stroke. Therefore, it is possible to determine the stress in the principle axis system.

Keywords: Finite Element Simulation, Several Plastic Deformation, Constrained Grooved Pressing, AZ31 Magnesium Alloys.

Classification numbers: 2.9.1, 4.10.4, 5.9.3.

1. INTRODUCTION

Motivated by the actual debate on the sustainable use of energy, materials scientists and engineers are seeking for possibilities to support efforts for lowering energy consumption. An ability to execute is to develop materials that allow structural design with retained functionality and strength at a lower weight. Consequently, the specific strength (i.e., strength of a material normalized to the mass density) becomes a key parameter for the materials' selection in

mechanical design. Strengthening mechanisms such as cold working and solid solution, dispersion, and precipitation hardening are adaptable to many metals. However, they are limited in their scale and the density is typically not affected at all. Furthermore, the ductility is usually reduced to a value well below the minimal requirements of the application.

It is well known that heavy cold (warm) deformation can result in significant refinement of the microstructure of metallic materials [1,2]. Based on this grain refinement effect, bulk nanostructured materials are processed by several methods of severe plastic deformation (SPD) [3 - 13]. A severe plastic deformation method with great potential for the production of ultrafine materials has been developed as a Constrained Grooved Pressing (CGP). In 2001, Zhu undertook a SPD method based on the method of squeezing a flat metal plate with a cyclic groove die and then restoring the original planar shape to the flat die [14]. Lee and Park [15] have continued to research and develop CGP technology, combining numerical simulation with experiments, the authors have researched and produced ultrafine grained materials with pure aluminum by CGP technology with cooled samples [16]. The team reported that the yield limit and strength of the material were significantly improved compared with experimental conditions at room temperature, but there was no significant difference in grain structure [17,18]. Peng *et al*. used CGP technology to study the change in mechanical properties of Cu-Zn alloy [19]. By numerical simulation method, *Yoon et al*. showed that the strain in the first compression is larger than in the second and subsequent compressions [20]. Zrnik *et al*. [21, 22] studied the deformation and change of material structure through CGP technology with aluminum sheet samples at normal temperature. Extensive twinning found also in almost (1, 2 and 3) areas of the specimen implied that twinning is prevalent mechanism of deformation at one complete CGP cycle [23] and microstructure and mechanical properties were analyzed for a material with ultra-fine grained structure prepared by CGP of AZ31 magnesium alloy [24,25]. Repetition of this process causes large plastic deformation to accumulate in the sample without significantly altering the initial size (Figure 1(a)). One of the main benefits of the CGP technique is the improvement of mechanical properties without any change in the size of the material.

The amount of plastic strain is dependent on the number of pressing (n) and die geometry such as groove angle under the plane strain shear deformation using the equation (1) of effective strain [14].

$$\varepsilon = n\frac{4}{\sqrt{3}} ln\left(\frac{r+t}{r+0.5t}\right) \; with \; r = \frac{t}{sin\theta} \tag{1}$$

where, n is the number of time, t is the thickness of the workpiece and θ is the groove angle.

The variation of the groove angle of the die to changes in the deformation level of the workpiece. Effective strain (ε_{eff}) is calculated by the following equation [26].

$$\varepsilon_{eff} = \frac{\tan\theta}{\sqrt{3}} \tag{2}$$

In this study the simulation of CGP plastic deformation process by finite element method allows us to determine technological parameters such as pressure force, stress field, strain field and risk of failure.

2. SIMULATIONS AND METHODS

2.1. Modeling and simulations

DEFORM can be used to analyze most thermo-mechanical forming processes, and many heat treatment processes. The general approach is to define the geometry and material of the

initial workpiece in DEFORM, then sequentially simulate each process that is to be applied to the workpiece. Flow stress data is compiled from a variety of sources and it is only provided as a reference data set. Material testing should be performed to obtain flow stress data for critical applications (Figure 2).

In the CGP simulation (shown in Figure 1(b)), the plate with geometry of (60 × 60 × 3) *mm* was modeled. The temperature of the workpiece and die are considered constant and equal to 200 °C. The pressing speed and coefficient of friction between the die and workpiece were taken to be 10 mm/s and 0.1, respectively.

Table 1. Numerical simulation of mechanical properties [27].

Properties	AZ31
Density, kg/m^3	1,77
Tensile Strength, MPa	275
Proof Stress (Yield Strength), MPa	190
Modulus of Elasticity, GPa	45
Poissons ratio	0,35

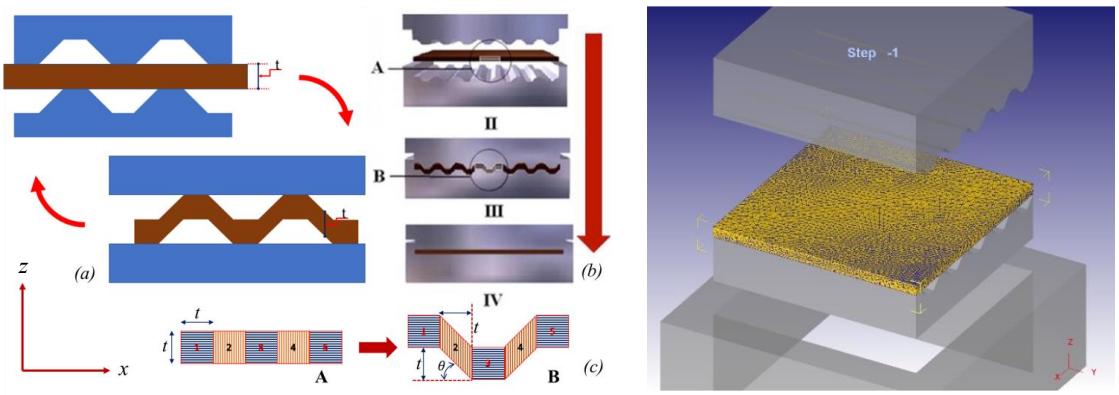

(a) *(b)*

Figure 1. Schematic representation of CGP process (a) and die and workpiece used in FEM simulation (b).

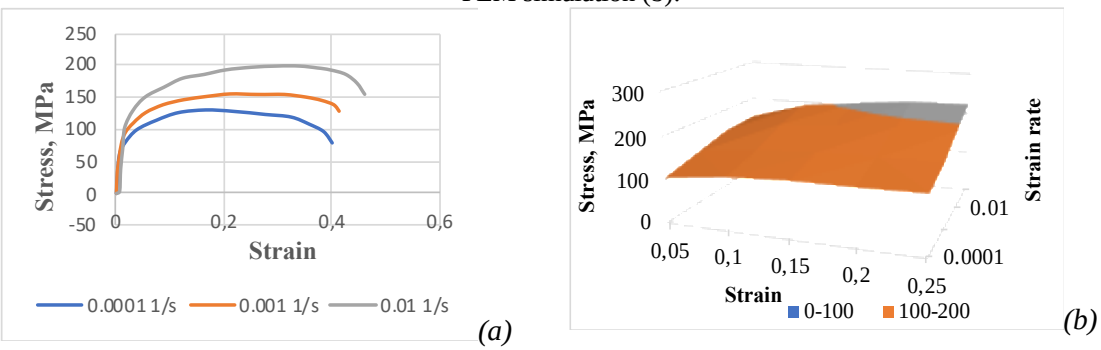

Figure 2. The effect of proof stress on ε and ε̇ at 200 °C [28].

2.2. Theoretical background

In the CGP process, the stress and strain of the workpiece can be analytically calculated with simplification but still remain the generality of the problem. Numerical simulation, which is a method of linearizing partial differential equations of plastic deformation problem, also has many errors but it can be used to compare with analytical calculation results. The workpiece is sheet-shaped and the friction flural on the surface of the workpiece in both directions Ox and Oy is large enough so that the workpiece does not expand and elongate. The deformation process of the workpiece in the CGP groove mold is divided into three stages as shown in Figure 3, depending on the working stroke of the upper die, as follows: (i) The first stage is elastic bending, when the die is in contact with the workpiece and the force creates moments at the top edge points of the mold groove. That reversing moments create tensile and compressive elastic on the workpiece as illustrated in Figure 3(a); (ii) The second stage is tensile combined with bending as shown in Figure 3(b). This tensile stress is combined with the bending stress to form a fan-shaped stress domain. The stress on the surface is massive which causes local deformation, and the reverse of tensile and compressive forces in the vicinity of the surface, causing the workpiece to be bent and wavy; (iii) The third stage is the compression process (Figure 3(b)), when the distance between the two sides is equal to the thickness of the workpiece t (Figure 1(a)) and ends when the distance is equal to $0.7t$. The strain in the compression process (the third stage) is more favorable than the tension (the second stage) because the crystal twining occurs when there is a favorable compressive stress.

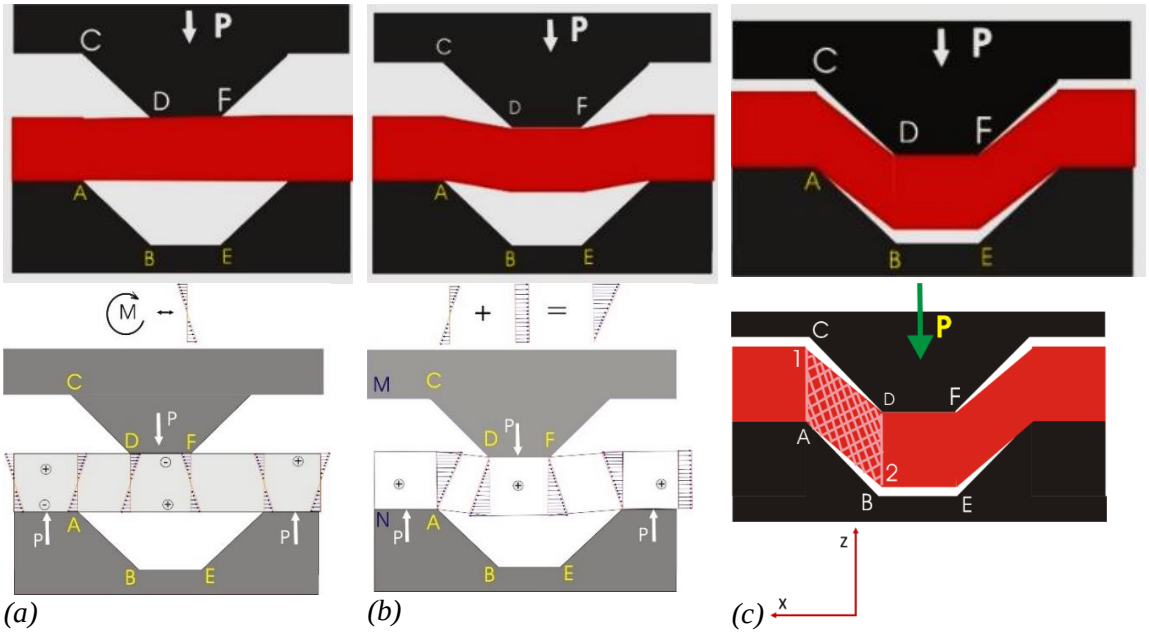

Figure 3. Three stages of CGP process and stress diagram of the workpiece: (a) bending, (b) tension and (c) compression.

In the case of flat pressing, if the force is not large enough, the pressure marks on the workpiece surface still exist. The deformation process is also referred to the single slip process. The system of equations for the plastic deformation problem in the condition of plane deformation is written as follows [29]:

$$\begin{cases} \frac{\partial \sigma_{xx}}{\partial x} + \frac{\partial \tau_{xz}}{\partial z} = 0 \\ \frac{\partial \tau_{xz}}{\partial x} + \frac{\partial \sigma_{zz}}{\partial z} = 0 \end{cases} \quad (3)$$

$$(\sigma_{xx} - \sigma_{zz})^2 + 4\tau_{xz}^2 = 4k^2 \quad (4)$$

Equation (3) is a balanced equation, Equation (4) is the plastic condition for the flat strain state.

Based on the properties of the slides, we can build a slide system in the deformation zone of the workpiece. Based on the boundary conditions, we calculate the stress at any point in the deformation region, depending on the hydrostatic stress and the rotation angle of the slide.

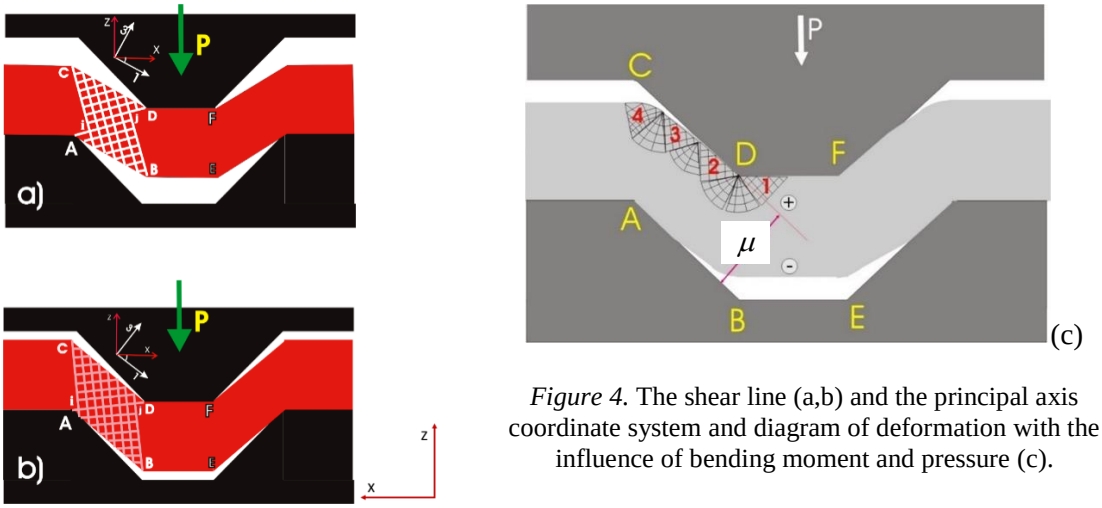

Figure 4. The shear line (a,b) and the principal axis coordinate system and diagram of deformation with the influence of bending moment and pressure (c).

It is assumed that in the workpiece there is no transition zone between the deformed and undeformed domain, specifically, there is no radius of curvature as shown in Figure 4(a,b). The slide field is created based on the consequences of the properties, specifically, the slides extend beyond the free boundary surface ($\mu = 0$) when an angle of 0 and the contact boundary has sticky friction ($\mu = 1$) under an angle of -45 ° (x axis). Therefore, we can determine the slide field, the stress distribution on the contact surface between the metal and the mold to calculate the pressure. Therefore, some studies [30] suggest that the workpiece is pressed between the two inclined faces of the mold in stage 3 as shown in Figure 4(c).

Due to the combination of bending moment, tensile force and compressive force in stage 3, it creates a plastic deformation area and there is a continuous transition from the undeformed zone to the plastic deformation zone. Plastic deformation occurs locally in different regions, with an elongation and a compression zone. Based on the sliding speed chart, it is possible to approximate the contact stress between the mold and the workpiece as well as the pressing force. Due to the complexity of analytically solving nonlinear theoretical problems, numerical modeling and simulation methods will be added to clarify the problem. In order to achieve a high degree of simulation accuracy, it is important to understand the material properties required to specify materials in DEFORM [31]. The material properties that the user is required to specify should contain typical functions needed for utilizing in the simulation. For studying the plastic deformation behavior of a given metal it is appropriate to consider uniform or homogeneous deformation conditions. The yield stress of a metal under uniaxial conditions as a function of strain ($\bar{\boldsymbol{\varepsilon}}$), strain rate ($\dot{\bar{\boldsymbol{\varepsilon}}}$), and temperature ($T$) can also be considered as flow stress. The metal

starts flowing or deforming plastically when the applied stress reaches the value of yield stress or flow stress.

$$\bar{\boldsymbol{\sigma}} = \bar{\boldsymbol{\sigma}}\left(\bar{\boldsymbol{\varepsilon}}, \dot{\bar{\boldsymbol{\varepsilon}}}, \boldsymbol{T}\right) \quad (\mathbf{6})$$

where $\bar{\boldsymbol{\sigma}}$, flow stress, $\bar{\boldsymbol{\varepsilon}}$, effective plastic strain, $\dot{\bar{\boldsymbol{\varepsilon}}}$, effective strain rate and *T*, temperature.

The material model in the general case is built with many different experimental equations, with many characteristic constants for material properties variation. In equation (7) of isothermal forming technology, yield stress is calculated through n and m.

$$\bar{\sigma} = K\varepsilon^n \dot{\varepsilon}^m, when\ n = 0 \rightarrow \bar{\sigma} = K\dot{\varepsilon}^m \quad (7)$$

Then, the sensitivity of stress to strain rate *m* is determined by the equation: $\boldsymbol{m} = \boldsymbol{\partial \ln \sigma / \partial \ln \dot{\varepsilon}}$ [32]. The influence of strain rate on yield stress is shown through many different models. The strain strength exponentiation *n* and the sensitivity coefficient of yield stress to the strain rate *m* are determined experimentally ($\mathbf{0} \leq \boldsymbol{m, n} \leq \mathbf{1}$), depending on the texture, structural function, thermomechanical conditions, and strain history, they are used in equations for determining yield stress of materials.

3. RESULTS AND DISCUSSION

The plastic deformation zone in CGP is not directly affected by stress from the die but through adjacent zones of the die, called the contact zone. The complexity of the process is the alternation of plastic deformation between the two zones (*ACDB* and *BDFE* in Figure 4). It creats an interface - a contact buffer between elastic and plastic deformation. Moreover, at the same time, the deformation is in opposite directions (top tension and bottom compression or vice versa) due to influence of bending moment.

Every CGP cycle consists of 4 passes and 9 steps [25]. In the 1st pass (1-2), a specimen is placed in the die with slight gap which is equal to the sheet thickness (1) and groove pressing begins (2). In the 2nd pass (3-4), flat pressing occurs (3); after that the specimen is rotated by 180 ° around the *z* direction and the groove pressing is repeated (4). In the 3rd pass (5-6), flat pressing occurs and is followed by a move of *t* to the right (5) and then a groove pressing (6). In the 4th pass (7-8), flat pressing occurs (7); after that the specimen is rotated by 180 ° around the *x* direction and moved to the left and the groove pressing is repeated (8). Finally, the specimen is flattened again and rotated by 180 ° around the *z* direction (9) and the groove pressing of the next cycle is started (1). In general, the cycle end points return to the initial position, with negligible deviations, indicating that the pressing process keeps the original shape of the workpiece and the deformation occurs relatively evenly. This study diagram also shows a huge difference between the two ideal and real cases. The bending, tension and compression stages are always present by the movement from the die contact zone to the deformation zone.

Figure 5(a) shows the equivalent strain distribution on the surface of the workpiece from the middle P1 of the first contact zone to the middle P5 of the second contact zone. Points P1 and P5 are the compression and tension with equal absolute values because of symmetry .It shows that at the end of ¼ cycle at the contact zone there is also a significant plastic deformation. The point P2 is tensed and P4 is compressed on the interface between the two deformation zones, whose strain is very large, but still smaller than the point P3 of the deformation zone. This is due to the influence of the contact zone. Figure 5(b) shows the workpiece shape at the end of pressing process with the deformation degree of five different points. At points P1 and P5 there is no deformation of the transition zone. At points P2 and P4,

the boundary between the two zones has half of the deformation in the zone middle. In conclusion, the boundary area will be further deformed in the second half of the cycle. At the end of each cycle, there will be a balance of strain for the entire section of the workpiece.

Figure 6(a) shows the contact and non-contact stresses that cause shear deformation on the surface. The stress point P3 (compression zone) and of point P4 (compression angle) are the largest level, which will cause severe deformation. At points P1, P2 and P5 on the free surface and sticky friction, the shear stress has a smaller value, the point P2 has a higher value because of bending moment. The maximal principal stress distribution in Figure 6(b) shows three different stages of the process: bending, tension and compression. In the first two stages, the stresses at the respective points P1 ÷ P5 are small, with negligible deviation between positive and negative values. In the compression stage, they are much different from each other, gradually increasing from the transition zone to the plastic deformation zone and especially spike at the end of the stroke when filling the die cavity. The maximal principal stress value has a direct effect on the hydrostatic stress that keeps the workpiece non-destructive under severe deformation.

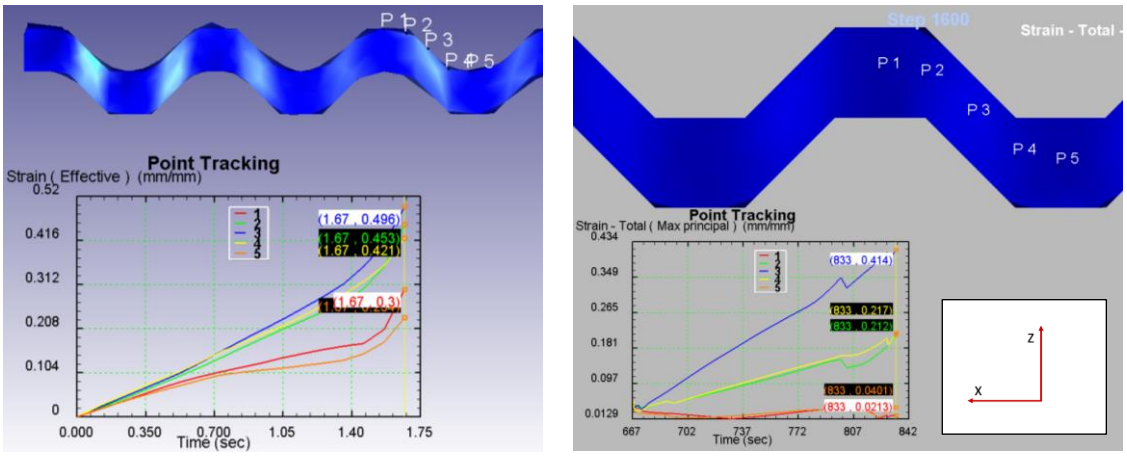

(a) *(b)*

Figure 5. Comparison of effective strain on the contact surface (a) and the center (b) of the workpiece during CGP process.

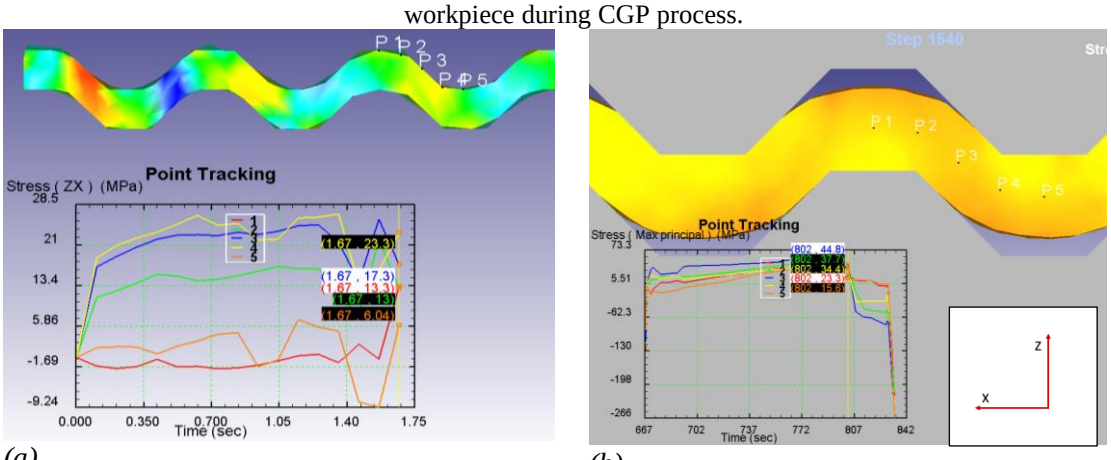

(a) *(b)*

Figure 6. Shear stress in the *ZX* plane (a) and distribution of the max principal stress (b) on the center of the workpiece.

The distribution of the workpiece shear stress at the beginning of the first cycle at the boundary line between the two zones in the *ZX* plane is shown in Figure 7(a). The boundary zone is subjected to a complex applied force, varying from positive to negative during the same groove and flat pressing, but the shear stress causes relatively uniform shear deformation throughout the stroke.

Figure 7(b) is the distribution of strain of the workpiece on the boundary line between the two zones in cycle 4. The cumulative deformation level is 474 %, the deviation on the thickness is not significant, about 7 % compared to the initial. At this point, the material plasticity and the strain behavior have changed. Specifically, when compressed, the metal hugs the die surface. The free surface when bending is evenly rounded. Based on the contact diagram between the die and the workpiece, the deformation zone is divided into three subzones, which is very clearly reflected in the numerical simulation results through the background colour.

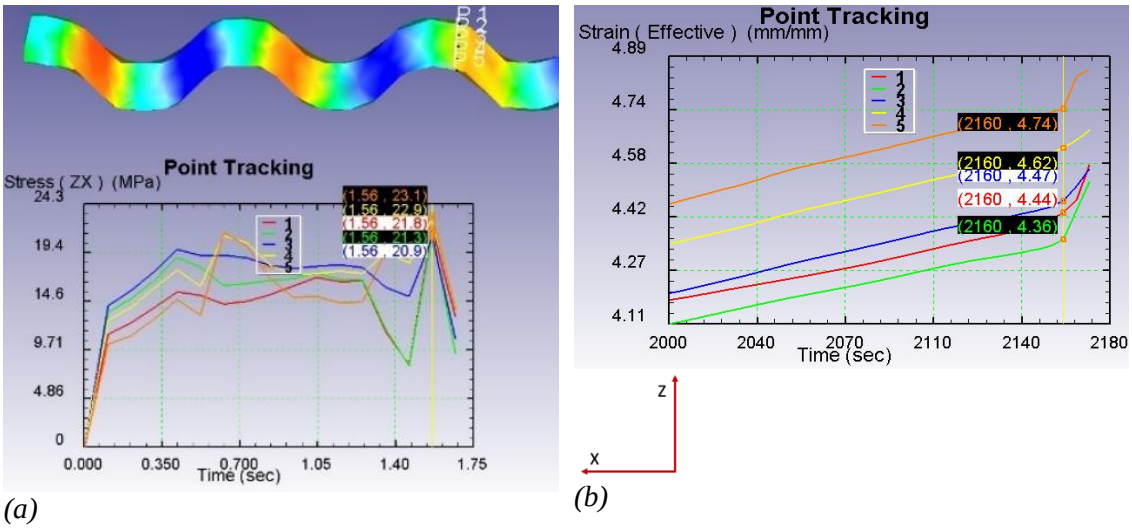

(a) *(b)*

Figure 7. Distribution shear stress (a) and strain (b) of the workpiece at the position between the deformed and undeformed zones.

Through the analytical method [33] based on equation (1), it is possible to determine the plastic strain of the workpiece during the pressing process, thereby to calculate the Von Mises equivalent strain from the equation. Strains during simulation have approximate results as calculated by the theory [34].

The simulated equivalent strain is higher than the theoretical value possible due to oversimplified assumptions and possible errors. Indeed, the friction coefficient, and thus the principal axes of coordinate system are not accurately determined, so the component values of stress and strain tensors have errors. In fact, the workpiece has a complex coherent 3D stress state, which changes the plastic deformation accumulation process. Diverse research results of some authors are explained by different boundary conditions. In the process of flat pressing of the sample, more plastic deformation is accumulated, the degree of plastic deformation occurs locally in the zones, reaching approximately 1.16 [24].

Figure 8(a) shows that during the flat pressing process, the shear stress has a stable value during uniform deformation. Similar to the groove pressing process, the effect diagram of stress during flat pressing includes compressive stress combined with bending stress of moment but in

opposite directions. Although the deformation zone has free surfaces controlled at both ends, the shear deformation is still uniform. This is possible because the workpiece thickness is thin, the pitch is small, and an inclination angle of 45 ° of the groove is large enough. After deformation, the workpiece surface is not wrinkled. The advantage of the deformation process in flat pressing is that the state of compressive stress occurs during the process. The stress change graph also shows the effect of direct and reverse elastic deformation at the beginning and the end of the stroke, when the pressure increases linearly. Step 3840 in Figure 8(b) is the second flattening process of cycle 3, when the mechanical properties of the material have improved, the hydrostatic stress is also much higher than that of the first cycle.

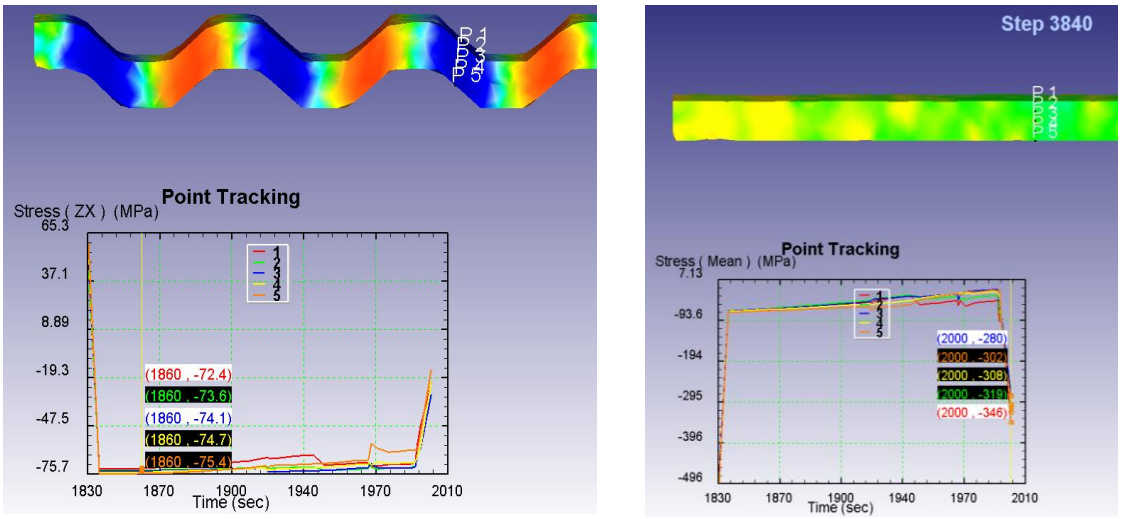

(a) *(b)*

Figure 8. Shear stress (a) and hydrostatic stress (b) during flat pressing.

Figures 9(a) and (b) show that although the deformation zone alternates the transition zones discontinuously, after each cycle the deformation throughout the workpiece is uniform. Especially after the first cycle, the workpiece has been rotated by an angle $\omega_Z = 180$ °, so the anisotropy of the workpiece is observed.

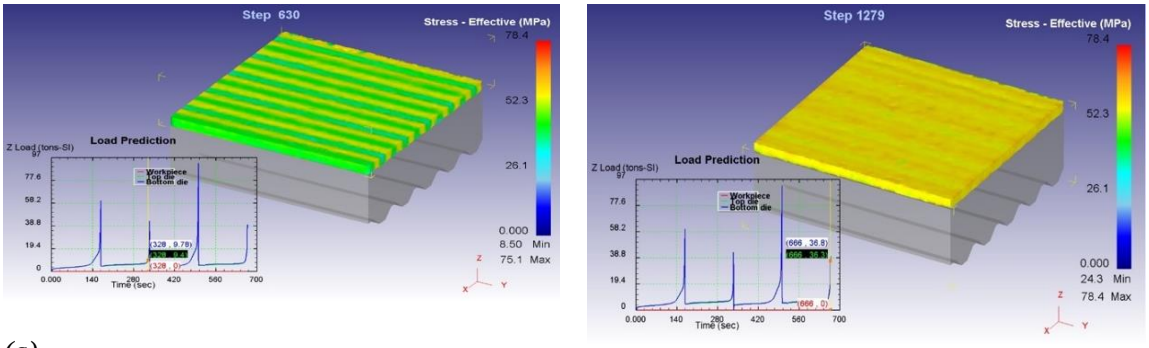

(a) *(b)*

Figure 9. The simulation results of flat pressing after the first half of cycle 2 (a) and after two cycles (b).

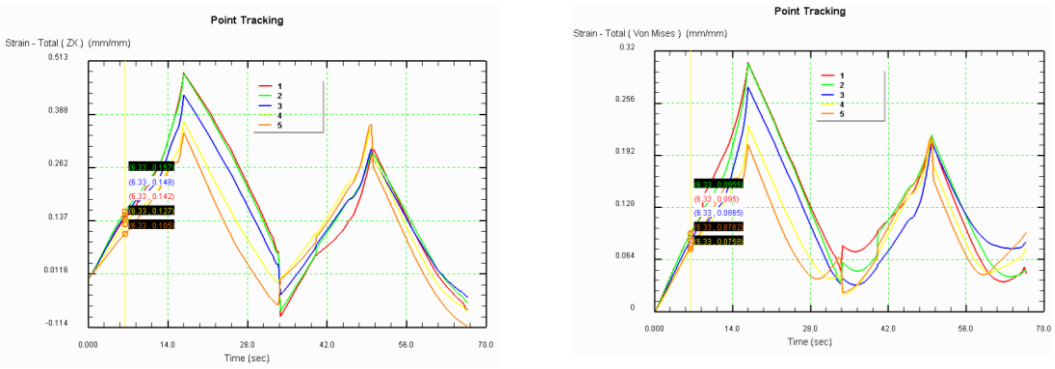

Figure 10. Shear strain in the *ZX* plane and von Mises strain in the transition zone of the workpiece.

Figures 10(a) and (b) have the same values, showing that the total strain of the workpiece is mainly the shear strain performed in the *ZX* plane. Since the deformation process is divided into several reverse pressing stages, the deformation values change sign. However, the total strain is still accumulated to high values.

4. CONCLUSIONS

Numerical simulation of CGP plastic deformation process by finite element method allows to determine technological parameters such as compressive force, stress field, deformation field and risk of failure or destruction.

The stress-strain state has been analyzed at the characteristic points of the plastic deformation zone including on the surface, at the center of the workpiece and at the transition zones, the results are consistent with the theoretical study. The unique feature of CGP technology compared to other types of SPD shows that the plastic deformation zone is not in direct contact with the die surface, but subjected to indirect forces, and has a small hydrostatic stress. The hydrostatic force and stress parameters only take effect at the end of the backlash de-elastic compression stroke.

The small coefficient of friction reduces the shear deformation intensity but increases the die filling capacity and the uniformity of the deformation process. However, because the contact surface between the workpiece and the die is large enough, the friction force can still control the deformation in the longitudinal and transverse directions of the workpiece. It keeps the deformation diagram flat and creates a high hydrostatic pressure effect that prevents the workpiece from being destroyed when deformed.

Through numerical simulation, it is possible to visually determine the state of stress and strain on the entire workpiece at all times of the stroke. Therefore, it is possible to determine the stress in the principle axis system.

Acknowledgements. This research was supported by the Vietnam National Foundation for Science and Technology Development (NAFOSTED) No. 107.01-2018.25.

CRediT authorship contribution statement. Author 1: Writing - Original Draft, Data analysis, Methodology, Review and Editing, Supervision, Funding acquisition. Author 2 and 3: Conceptualization, Data analysis, Methodology. Author 4 and 5: Data analysis, Methodology. Author 6: Supervision, Review and Editing.

Declaration of competing interest. The authors declare that they have no known competing financial interests or personal relationships that could have appeared to influence the work reported in this paper.

REFERENCES

1. Tsuji N. - Bulk Nanostructured Materials (Eds: M. J. Zehet- bauer , Y. T. Zhu), WILEY-VCH, Weinheim, 2009, pp. 235.
2. Valiev R. Z., Islangeliev R. K., Alexandrov I. V. - Russian Federration, 1999.
3. Valiev R. Z., Langdon T. G. - Principles of Equal- Channel Angular Pressing as a Processing Tool for Grain Refinement, Progress in Materials Science **51** (7) (2006) 881-981. doi:10.1016/j.pmatsci.2006.02.003
4. Segal V. M. - Materials processing by simple shear, Mater. Sci. Eng. A **197** (1995) 157-164. doi.org/10.1016/0921-5093(95)09705-8
5. Baik S. C., Estrin Y., Kim H. S., Hellmig R., and Jeong H. T. - Calculation of deformation behavior and texture evolution during equal channel angular pressing of IF steel usingdislocation based modeling of strain hardening, Mater. Sci. Forum **408-412** (2002) 697-702.
6. Kim H. S. - Prediction of temperature rise in equal channel angular pressing, Mater. Trans. **42** (2001) 536-538. doi.org/10.2320/matertrans.42.536.
7. Fukuda Y., Oh-ishi K., Horita Z., and Langdon T. G. - Processing of a low-carbon steel by equal-channel angular pressing, Acta Mater. **50** (2002) 1359-1368.

   doi.org/10.1016/S1359-6454(01)00441-4
8. Kim H. S., Lee Y. S.,. Hong S. I, Tarakanova A. A., and Alexandrov I. V. - Deformation behavior of copper during a high pressure torsion process, J. Mater. Proc. Technol. **142** (2003) 334-337. https://doi.org/10.1016/S0924-0136(03)00590-9
9. Faraji G., Mashhadi M. M., and Kim H. S.- Tubular channel angular pressing (TCAP) as a novel severe plastic deformation method for cylindrical tubes, Mater. Lett. **65** (2011) 3009-3012. https://doi.org/10.1016/j.matlet.2011.06.039
10. Kim H. S., Quang P., Seo M. H., Hong S. I., Baik K. H., and Nghiep D. M. - Process Modelling of Equal Channel Angular Pressing for Ultrafine Grained Materials Materials Transactions, **45** (7) (2004) 1-5. https://doi.org/10.2320/matertrans.45.2172
11. Quang P. and Hao P. T. - The Preparation and Characterization of Cu/AA6061 multi-layer Composte produced by Accumulated Roll Bonding, IOP Conf. Series: Materials Science and Engineering **758** (2020) 012099 doi:10.1088/1757-899X/758/1/012099
12. Xu C., Furukawa M., Horita Z., and Langdon T. G. - The evolution of homogeneity and grain refinement during equal-channel angular pressing: A model for grain refinement in ECAP, J. Mater. Sci. Eng. A, **398** (2005) 66-76.

    https://doi.org/10.1016/j.msea.2005.03.083
13. Zhu Y. T., Lowe T. C., Jiang H.and Huang J. - Patent No. 6197129, USA, 2001.
14. Lee P. J. - Numerical and experimental investigations of constrained groove pressing and rolling for grain refinement, J. Mater. Process. Technol, **130-131** (2001) 208-213.

15. Krishnaiah I., Chakkingal U., and Venugopal P. - Production of Ultrafine Grain Sizes in Aluminium Sheets by Severe Plastic Deformation Using the Technique of Groove Pressing, Scripta Materialia **52** (2005) 1229-1233.
16. Krishnaiah A., Chakkingal U., Venugopal P., - Applicability of the groove pressing technique for grain refinement in commercial purity copper, Mater Sci. Eng. A **410-411** (2005) 337-40.
17. Peng K., Su L., Shaw L., Qian K. - Grain refinement and crack prevention in constrained groove pressing of two-phase Cu-Zn alloys, Scr. Mater. **56** (2007) 987-90.
18. Yoon S. C., Krishnaiah A., Chakkingal U., Kim H. S. - Severe plastic deformation and strain localization in groove pressing, Comput Mater Sci. **43** (2008) 641-5.
19. Zrnik J., Kovarik T., Novy Z., Cieslar M. - Ultrafine-grained structure development and deformation behavior of aluminium processed by constrained groove pressing, Mater Sci. Eng. A **503** (2009) 126-9.
20. Aal M., Kim H. S. - Wear properties of high pressure torsion rocessed ultrafine grained Al-7%Si alloy, Mater Des. **53** (2014) 373-82.
21. Quang P., Thuy P. T., Hue D. T. H., Ngung D. M., Schukin V. Y. - The deformation of AZ31 magnesium alloy during warm constrained groove pressing Acta Metallurgica Slovaca **25** (1) (2019) 48-54. DOI 10.12776/ams.v25i1.121
22. Thuy P. T., Hue D. T. H., Ngung D. M., and Quang . - Evolution of microstructure and mechanical properties of magnesium alloy AZ31 after Constrained Groove Pressing, J. Science and Technology of Metals (78) (2018) 32-36.
23. Thuy P. T., Hue D. T. H., Ngung D. M., and Quang P. - A Study on Microstructure and Mechanical Properties of AZ31 Magnesium Alloy after Constrained Groove Pressing IOP Conf. Ser.: Mater. Sci. Eng. **611** (2019) 012005.

    doi:10.1088/1757-899X/611/1/012005
24. Zhu, Y.T., Jiang, H., Huang, J. et al. - A new route to bulk nanostructured metals, Metall Mater. Trans. A **32** (2001) 1559-1562. https://doi.org/10.1007/s11661-001-0245-0
25. Brandes E. A. - Smithells metals reference book, Butterworths, 1988.
26. Cheng Y. Q., Zhang H., Chen Z. H., Xian K. F., - Flow stress equation of AZ31 magnesium alloy sheet during warm tensile deformation, Journal of materials processing technology **208** (2008) 29-34. https://doi.org/10.1016/j.jmatprotec.2007.12.095.
27. Brandes E. A. - Smithells metals reference book, Butterworths, (1988).
28. Cheng Y. Q., Zhang H., Chen Z. H., Xian K. F., - Flow stress equation of AZ31 magnesium alloy sheet during warm tensile deformation, Journal of materials processing technology **208** (2008) 29-34. https://doi.org/10.1016/j.jmatprotec.2007.12.095
29. Storozhev M. V., Popov E. A. - Theory of metal forming, Publishing House, Mechanical Engineering, Moscow, 1971.
30. Smirnov O. M. - Processing of metals by pressure in the state of superplasticity - M., Mashinostroyeniye, 1979, pp. 184.
31. Vratna J. - Physical Properties of Ultrafine-grained Polycrystals of Magnesium Based Alloys, DIPLOMA THESIS, 2010, pp. 6-7.

32. Fong K. S., Atsushi D., Jen T. M., Chua B. W. - Effect of deformation and temperature paths in severe plastic deformation using groove pressing on microstructure, texture, and mechanical properties of AZ31-O, J. Manuf. Sci. Eng. **137** (5) (2015) 051004. https://doi.org/10.1115/1.4031021